Anharmonic Models and Thermal-Expansion Calculations for KBr†

Robert J. Hardy
Behlen Laboratory of Physics, University of Nebraska, Lincoln, Nebraska 68508

Arnold M. Karo
Lawrence Livermore Laboratory, University of California, Livermore, California 94550

(Received 18 August 1972)

The mode-Grüneisen parameters, the macroscopic Grüneisen function $\gamma(T)=3\alpha B^{is} V/C_V$, and the coefficient of thermal expansion α are calculated for KBr. Three anharmonic models are used: the rigid-ion (RI) model, a deformation-dipole (DD) model in which the deformability of the ions does *not* depend on the volume V, and a DD model in which the deformability does depend on V. Allowing the deformability to depend on V significantly improves the agreement with experiment. A definite minimum in the low-temperature values of $\gamma(T)$ is predicted by the DD models, but not by the RI model. The distance between nearest neighbors r at which the potential energy of the lattice has its minimum value is found self-consistently. This value of r is used in the determination of the derivatives of the short-range overlap potential $v(r)$. The force constants obtained differ significantly from those obtained by substituting room-temperature experimental data into formulas derived using the equilibrium condition. Significantly larger values for $\gamma(T)$ and α, which are in better agreement with the experimental results, are obtained by allowing for the temperature dependence of the zero-pressure values of B^{is} and r.

I. INTRODUCTION

Recently, results of several model calculations of the linear coefficient of thermal expansion $\alpha(T)$ and the macroscopic Grüneisen function $\gamma(T)$ for the alkali halide crystal have been reported in the literature.[1-5] Reasonable agreement with the experimental results has been obtained.

We have carried out model calculations of $\alpha(T)$ and $\gamma(T)$ for KBr while trying to minimize the number of approximations made once the interactions included in the model have been specified. We also investigated the significance of several approximations that are often made in such model calculations by comparing the predictions obtained with our model when these approximations are made with the predictions obtained when they are not made.

The macroscopic Grüneisen function is given by

$$\gamma(T) = 3\alpha B^{is} V/C_V , \qquad (1.1)$$

where B^{is} is the isothermal bulk modulus, C_V is the heat capacity at constant volume, and V is the volume. The quantity $\gamma(T)$ is related to the normal-mode frequencies ω_i and the mode-Grüneisen parameters γ_i by

$$\gamma(T)=\sum_i C_i(T)\gamma_i \Big/ \sum_i C_i(T) , \qquad (1.2)$$

where $C_i(T)$ is the heat capacity of the normal mode with frequency ω_i and the sum is over all normal modes. The self-energy corrections to the free energy are neglected here. Equation (1.2) is most accurate when the values used for ω_i and γ_i are the values appropriate to the volume of the crystal at the temperature and pressure being considered. An often made approximation is to use Eq. (1.2) but neglect the change in the values of ω_i and γ_i caused by the change in volume due to thermal expansion. To determine the significance of this approximation we used a consistent expansion of the Helmholz free energy to derive expressions for the zero-pressure values of the quantities on the right-hand side of Eq. (1.1). The expressions obtained involve the values of ω_i and γ_i at only one volume, the volume that minimizes the potential energy. When these expressions are substituted into Eq. (1.1), the resulting formula for $\gamma(T)$ contains several corrections to Eq. (1.2). We find that these corrections affect the calculated values of $\gamma(T)$ by as much as 9% and that they significantly improve the agreement with the experimental results.

The equilibrium condition, i.e., the condition that the electrostatic forces balance the short-range overlap forces, is utilized in the derivation of the formulas commonly used to determine the first two derivatives of the short-range overlap potential $v(r)$ from the bulk modulus and the nearest-neighbor separation r. Of course, these forces balance exactly only in the configuration that minimizes potential energy. Because of the anharmonic nature of the interionic forces and because of zero-point motion, this configuration is never realized in real alkali halide crystals at zero pressure. Nevertheless, the values of the first two derivatives of $v(r)$ are often determined by substituting room-temperature zero-pressure experimental data into these formulas. We find that the values of the

derivatives determined in this way differ by as much as 10% from the values determined by a consistent use of the formulas.

Most of our calculations have been done with the deformation-dipole (DD) model, which is a generalization of the rigid-ion (RI) model that allows for the polarization of the ions in the crystal by the internal electric fields and for the distortion of the negative ions by their motion relative to their six nearest neighbors. The anharmonic model considered in greatest detail allows for anharmonicity in the overlap forces, in the RI part of the electrostatic interaction, and in the deformability of the ions; we refer to it as the anharmonic-deformation-dipole (ADD) model. Using it, we obtain reasonable agreement with the experimental values for $\alpha(T)$ and $\gamma(T)$ without the use of adjustable parameters. For comparison, we have also used a simpler-deformation-dipole model (SDD) that allows for anharmonicity in only the RI part of the dynamical matrix. We find that the predictions of the ADD model are in considerably better agreement with the experimental data than those of the SDD model. We also carried out anharmonic calculations with the RI model and found no low-temperature minimum in the values of $\gamma(T)$ predicted with it. The values of $\gamma(T)$ predicted with the ADD and SDD models do possess low-temperature minima.

II. THERMODYNAMICS

A. Helmholz Free Energy

The connection between the macroscopic thermodynamic properties of a system and its microscopic structure is made by the statistical mechanical formula for the Helmholz free energy:

$$F = -k_B T \ln(\mathrm{Tr}\, e^{-H/k_B T}) , \tag{2.1}$$

where H is the Hamiltonian of the system and k_B and T are Boltzmann's constant and the absolute temperature.

When applying Eq. (2.1) to a crystal lattice, one expands the potential-energy part of the Hamiltonian in a Taylor series of powers of the displacements of the ions from the positions they occupy when the potential energy is minimized. If the cubic terms in this series expansion are considered to be of order λ and the quartic terms are considered to be of the order λ^2, the perturbation expansion for the Helmholz free energy *per unit cell* through order λ^2 has the form

$$f(T,u) = f^{(0)}(T) + u f^{(1)}(T) + (u^2/2)[f^{(2)}(T) + \phi^{(2)}] + (u^3/3!)\,\phi^{(3)} + (u^4/4!)\,\phi^{(4)} . \tag{2.2}$$

In general the strain parameter u in Eq. (2.2) is a tensor. However, when considering the thermal expansion of cubic crystals, it is sufficient to consider the scalar strain parameter

$$u = (r - r_{\mathrm{pm}})/r_{\mathrm{pm}} , \tag{2.3}$$

where r is the distance between the average positions of nearest neighbors and r_{pm} is the potential-minimum value of r. The phrase "potential-minimum" is used to refer to the configuration of the lattice that minimizes the potential energy.

The coefficients $\phi^{(n)}$ in Eq. (2.2) are defined as

$$\phi^{(n)} = \left.\frac{d^n\phi}{du^n}\right|_{u=0} = (r_{\mathrm{pm}})^n \frac{d^n\phi(r_{\mathrm{pm}})}{dr^n} , \tag{2.4}$$

where $\phi(r)$ is the potential energy per unit cell associated with a collection of static ions with a distance r between nearest neighbors. Since the derivatives in Eq. (2.4) are evaluated at the potential-minimum value of r, it follows that $\phi^{(1)} = 0$.

The term $f^{(0)}(T)$ in Eq. (2.2) is given by

$$f^{(0)}(T) = \tfrac{1}{4} k_B T \left(\frac{r_{\mathrm{pm}}}{\pi}\right)^3 \sum_s \int d^3k \ln\left(2\sinh\frac{\hbar\omega_{\vec{k}s}}{2k_BT}\right) + \text{anharmonic terms}, \tag{2.5}$$

where $\omega_{\vec{k}s}$ is the frequency of the normal mode with wave vector $\vec{k}$ and polarization index s. All $\vec{k}$-space integrations are to be taken over the first Brillouin zone. Only the harmonic (i.e., $\lambda = 0$) term is given explicitly. The coefficient $f^{(1)}(T)$ in Eq. (2.2) is given by

$$f^{(1)}(T) = -3(2r_{\mathrm{pm}}^3)\,P_{\mathrm{th}}(T) = -\frac{3}{4}\left(\frac{r_{\mathrm{pm}}}{\pi}\right)^3 \sum_s \int d^3k \coth\frac{\hbar\omega_{\vec{k}s}}{2k_BT}\,\frac{1}{2}\,\hbar\omega_{\vec{k}s}\gamma_{\vec{k}s} , \tag{2.6}$$

where $P_{\mathrm{th}}(T)$ is the "thermal pressure," which is the pressure needed at temperature T to prevent the crystal from expanding beyond its potential-minimum volume, that is, its volume when $u = 0$. The mode-Grüneisen parameters are defined as

$$\gamma_{\vec{k}s} = -\frac{V}{\omega_{\vec{k}s}}\frac{\partial\omega_{\vec{k}s}}{\partial V} , \tag{2.7}$$

where the product $|\vec{k}|r$ is held constant in the differentiation. The volume V is related to r and to the strain u by

$$V = V_{\mathrm{pm}}(r/r_{\mathrm{pm}})^3 = V_{\mathrm{pm}}(1+u)^3 , \tag{2.8}$$

where V_{pm} is the potential-minimum value of V. Potential-minimum values for the frequencies and mode-Grüneisen parameters are required in Eqs. (2.5) and (2.6).

The terms in Eq. (2.2) containing the coefficients $\phi^{(n)}$ give the contributions to the free energy that result from the potential energy associated with a lattice having a distance r between the average positions of nearest neighbors. The terms containing the coefficients $f^{(n)}(T)$ gives the contributions that result from the motion of the ions about

their average positions. The harmonic part of $f^{(0)}(T)$ is simply the free energy per unit cell of a set of independent harmonic oscillators with frequencies $\omega_{\vec{k}s}$. The strain-dependent terms $uf^{(1)}(T)$ and $\frac{1}{2}u^2f^{(2)}(T)$ are the quasiharmonic contributions to the free energy which account for the dependence of the force constants (and thus the frequencies) on the average distance between nearest neighbors. The anharmonic terms in $f^{(0)}(T)$ are the self-energy contributions to the free energy.

B. Determination of Coefficients in Eq. (2.2)

In this article we use the anharmonic models described in Sec. III to determine $f^{(1)}(T)$ and the harmonic part of $f^{(0)}(T)$. We neglect the anharmonic terms in $f^{(0)}(T)$ and determine $f^{(2)}(T)$, $\phi^{(2)}$, and $\phi^{(3)}$ from the known temperature and pressure dependence of the bulk modulus. Since we lack a convenient experimental parameter with which to determine $\phi^{(4)}$, we make the simplifying assumption that

$$\phi^{(4)} = 0 . \tag{2.9}$$

We have approximated the temperature dependence of the zero-pressure isothermal bulk modulus $B_0^{is}(T)$ with the function

$$B_0^{is}(T) = B_{pm} + B_1 \coth(\theta_b/T) , \tag{2.10}$$

where the subscript 0 indicates zero pressure. The potential-minimum value of the bulk modulus, B_{pm}, was set equal to the ordinate of the intercept with the $T = 0$ axis of the straight-line extrapolation of the high-temperature experimental values of $B_0^{ad}(T)$ on a $B_0^{ad}(T)$-vs-T plot. $B_0^{ad}(T)$ is the zero-pressure adiabatic bulk modulus. The sum $B_{pm} + B_1$ was set equal to the experimental value of B_0^{ad} at 0 °K, which is also the 0 °K value of B_0^{is}. Experimental values for $B_0^{ad}(T)$ were obtained from Galt[6] and Sharko and Botaki.[7] The parameter θ_b was determined so that when Eq. (2.10) was evaluated at 300 °K it gave the value of B_0^{is} given by Reddy and Ruoff.[8] The values obtained were $B_{pm} = 1.772 \times 10^{11}$ dyn/cm^2, $B_1 = -3.2 \times 10^9$ dyn/cm^2, and $\theta_b = 27.9$ °K.

The thermodynamic expression relating the isothermal bulk modulus to pressure P, volume V, and free energy F is

$$B^{is} = -V\left(\frac{\partial P}{\partial V}\right)_T = V\left(\frac{\partial^2 F}{\partial V^2}\right)_T . \tag{2.11}$$

It follows from this and from Eq. (2.2) that at zero pressure

$$B_0^{is}(T) = \frac{\phi^{(2)} + f^{(2)}(T) + u_0(T)\,\phi^{(3)} + \frac{1}{2}u_0(T)^2\,\phi^{(4)}}{18 r_{pm}^3 [1 + u_0(T)]} , \tag{2.12}$$

where $u_0(T)$ is the zero-pressure value of the strain at temperature T. Rearranging the terms in Eq. (2.12) gives

$$\phi^{(2)} + f^{(2)}(T) = 18 r_{pm}^3 [1 + u_0(T)] B_0^{is}(T) - u_0(T)\,\phi^{(3)} - \tfrac{1}{2}u_0(T)^2\,\phi^{(4)} . \tag{2.13}$$

We have determined $\phi^{(2)}$ and $f^{(2)}(T)$ by substituting Eq. (2.10) into this and separately equating the temperature-independent and temperature-dependent terms from the two sides of the resulting equation. This gives

$$\phi^{(2)} = 18 r_{pm}^3 B_{pm} \tag{2.14}$$

and

$$f^{(2)}(T) = 18 r_{pm}^3 \{[1 + u_0(T)] B_1 \coth(\theta_b/T) + u_0(T) B_{pm}\} - u_0(T)\,\phi^{(3)} - \tfrac{1}{2}u_0(T)^2\,\phi^{(4)} . \tag{2.15}$$

It also follows from Eq. (2.11) that the isothermal pressure derivative of the bulk modulus at zero pressure is given by

$$\left(\frac{\partial B^{is}}{\partial P}\right)_T = 1 - \frac{\phi^{(3)} + u_0(T)\,\phi^{(4)}}{54 r_{pm}^3 B_0^{is}(T)} . \tag{2.16}$$

From this it follows that

$$\phi^{(3)} = 54 r_{pm}^3 B_0^{is}(T)\left[1 - \left(\frac{\partial B^{is}}{\partial P}\right)_T\right] - u_0(T)\,\phi^{(4)} . \tag{2.17}$$

This expression with $\phi^{(4)} = 0$ was used to determine $\phi^{(3)}$ from the 300 °K experimental values of B_0^{is} and of $(\partial B^{is}/\partial P)_T$ given by Reddy and Ruoff.[8]

To complete the determination of $f^{(2)}(T)$, the zero-pressure strain $u_0(T)$ must be determined. It follows from Eq. (2.2) and the thermodynamic relation $P = -(\partial F/\partial V)_T$ that at zero pressure

$$0 = f^{(1)}(T) + u_0(T)[f^{(2)}(T) + \phi^{(2)}] + \tfrac{1}{2}u_0(T)^2\,\phi^{(3)} + [u_0(T)^3/3!]\,\phi^{(4)} . \tag{2.18}$$

By substituting Eq. (2.13) into this and setting $\phi^{(4)} = 0$, one obtains the quadratic equation

$$u_0(T)^2 [3B_0^{is}(T) - (\phi^{(3)}/12 r_{pm}^3)] + u_0(T)\,3B_0^{is}(T) - P_{th}(T) = 0, \tag{2.19}$$

which is the equation we have solved to determine $u_0(T)$.

III. ANHARMONIC MODELS

A. Description of Models

The familiar *rigid-ion* model treats an alkali halide crystal as a collection of massive charged ions held in place by long-range electrostatic forces balanced by short-range overlap forces. The ions are considered to have monopole moments of magnitude $\pm e$, where e is the magnitude of the charge on an electron. Two-body central overlap forces, which act between nearest neighbors and can be derived from a potential $v(r)$, are considered.

The *deformation-dipole* model is an extension of

the RI model. In addition to the monopole moments associated with the ions, dipole moments are included to account both for the polarization of the electron clouds of the ions by the internal electric fields in the crystal and for the distortion of the electron clouds by their motion relative to their six nearest neighbors. Polarization dipoles on both the positive and negative ions are included; deformation dipoles on only the negative ions are allowed for.

It follows from definition (2.7) and relation (2.8) between the volume and the nearest-neighbor distance that the mode-Grüneisen parameters are given by

$$\gamma_{\vec{k}s} = \frac{-r}{3\omega_{\vec{k}s}} \frac{\partial \omega_{\vec{k}s}}{\partial r} \quad . \tag{3.1}$$

The derivatives needed can be determined either with

$$\frac{\partial \omega_{\vec{k}s}}{\partial r}(r) = \frac{\omega_{\vec{k}s}(r+\Delta r) - \omega_{\vec{k}s}(r)}{\Delta r} \tag{3.2}$$

or with

$$2\omega_{\vec{k}s} \frac{\partial \omega_{\vec{k}s}}{\partial r} = E_{\vec{k}s} \cdot \frac{\partial \underline{D}}{\partial r} \cdot E_{\vec{k}s} \ , \tag{3.3}$$

where $E_{\vec{k}s}$ is the eigenvector of the dynamical matrix $\underline{D}_{\vec{k}}$ associated with the eigenvalue $\omega^2_{\vec{k}s}$:

$$\omega^2_{\vec{k}s} = E_{\vec{k}s} \cdot \underline{D}_{\vec{k}} \cdot E_{\vec{k}s} \ . \tag{3.4}$$

Equation (3.2) has been used with the ADD model, while Eq. (3.3) has been used with the RI model.

The dynamical matrix for the DD model can be expressed as

$$\underline{D}^{DD}_{\vec{k}} = \underline{D}^{RI}_{\vec{k}} + \underline{D}'_{\vec{k}} \ , \tag{3.5}$$

where $\underline{D}^{RI}_{\vec{k}}$ is the RI dynamical matrix and $\underline{D}'_{\vec{k}}$ is an additive term that accounts for the effects of the polarization and deformation dipoles. A simple way to allow for the dependence on r (or equivalently, on V) of both the nearest-neighbor force constants and the monopole part of the electrostatic interaction, while neglecting any r dependence in the strengths of polarization and deformation dipoles, is to calculate the mode-Grüneisen parameters using Eq. (3.3) with the derivative of the additive term $\underline{D}'_{\vec{k}}$ neglected. This gives

$$\gamma^{SDD}_{\vec{k}s} = \frac{-r}{6(\omega^{DD}_{\vec{k}s})^2} E^{DD}_{\vec{k}s} \cdot \frac{\partial \underline{D}^{RI}}{\partial r} E^{DD}_{\vec{k}s} \ , \tag{3.6}$$

where $E^{DD}_{\vec{k}s}$ and $(\omega^{DD}_{\vec{k}s})^2$ are the eigenvectors and eigenvalues of $\underline{D}^{DD}_{\vec{k}}$.

The anharmonic model that uses normal-mode frequencies determined with the DD model and mode-Grüneisen parameters determined with Eq. (3.6) will be referred to as the SDD model. This model is appealing for several reasons: (i) the expectation that the short-range forces are the major source of anharmonicity in an alkali halide crystal; (ii) the fact that the determination of the mode-Grüneisen parameters with Eq. (3.6) requires only one more input parameter than the calculation of the frequencies; and (iii) the fact that the expression for $\partial \underline{D}'/\partial r$ is much more difficult to evaluate than the expression for $\partial \underline{D}^{RI}/\partial r$.

Our most complete anharmonic model, which we call the ADD model, not only allows for the r dependence of the nearest-neighbor force constants and of the monopole part of the electrostatic interaction, but also allows for r dependence in the strength of the deformation dipoles. For simplicity we have assumed that the polarizabilities α_+ and α_- are independent of r.

B. Input Parameters

The essential input parameters needed for determining the normal-mode frequencies $\omega_{\vec{k}s}$ are listed in the top row of Fig. 1. The first and second derivatives $v'(r)$ and $v''(r)$ of the short-range potential and the average distance between nearest neighbors r are needed with both models. The electronic polarizabilities α_+ and α_-, the static dielectric constant ϵ_0, and the infrared dispersion frequency (or reststrahlung frequency) ω_0 are needed with the DD model only. The derivatives $v'(r)$ and $v''(r)$ are conventionally expressed in terms of the dimensionless parameters

$$B(r) = (4r^2/e^2)v'(r) \tag{3.7}$$

and

$$A(r) = (4r^3/e^2)v''(r). \tag{3.8}$$

The values of the input parameters used in determining the frequencies and mode-Grüneisen parameters are given in Table I.

C. Short-Range Potential $v(r)$

Values for $v'(r_{pm})$, $v''(r_{pm})$, and $v'''(r_{pm})$ are needed for the determination of the potential-minimum values of the frequencies and mode-Grüneisen parameters required in Eqs. (2.5) and (2.6). When Eq. (3.3) or Eq. (3.6) is used, $v'''(r_{pm})$ is

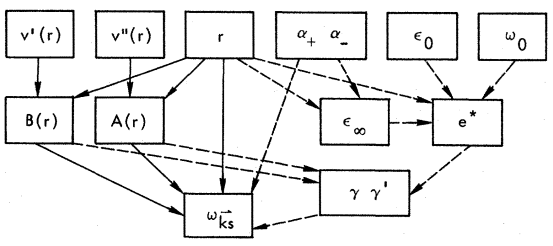

FIG. 1. Parameters needed for determining the normal-mode frequencies $\omega_{\vec{k}s}$ with the RI model (solid lines) and the DD model (solid and dashed lines).

TABLE I. Values of the input parameters used in determining ω_{fs} and γ_{fs} for KBr and the models in which the parameters are needed.

Parameter	Value	Model
$(4r_{pm}^2/e^2)v'(r_{pm}) = B(r_{pm})$	−1.165	ADD, SDD, RI
$(4r_{pm}^3/e^2)v''(r_{pm}) = A(r_{pm})$	12.82	ADD, SDD, RI
$(4r_{pm}^4/e^2)v'''(r_{pm})$	−116.4	ADD, SDD, RI
r_{pm}	3.2658×10^{-8} cm	ADD, SDD, RI
α_+	1.195×10^{-24} cm^3	ADD, SDD
α_-	4.109×10^{-24} cm^3	ADD, SDD
$(e^*/e)_{pm}$	0.7506	ADD, SDD
$(r_{pm}/e^*)(\partial e^*/\partial r)_{pm}$	2.937	ADD

needed to determine the derivative of the dynamical matrix. When Eq. (3.2) is used, values of $v'(r)$ and $v''(r)$ at $r = r_{pm} + \Delta r$ are needed, and they are given for small values of Δr by

$$v'(r_{pm}+\Delta r) = v'(r_{pm}) + v''(r_{pm})\,\Delta r \tag{3.9}$$

and

$$v''(r_{pm}+\Delta r) = v''(r_{pm}) + v'''(r_{pm})\,\Delta r\ . \tag{3.10}$$

In both the RI and DD models, the potential energy per unit cell $\phi(r)$ is related to the short-range potential $v(r)$ by

$$\phi(r) = -\alpha_M(e^2/r) + 6v(r)\ , \tag{3.11}$$

where α_M is Madelung's constant. Since $d\phi/dr$ vanishes when $r = r_{pm}$, it follows that

$$v'(r_{pm}) = -\frac{\alpha_M}{6}\frac{e^2}{r_{pm}^2}\ . \tag{3.12}$$

It also follows from Eq. (3.11) that

$$v''(r_{pm}) = \frac{1}{6r_{pm}^2}\phi^{(2)} + \frac{\alpha_M}{3}\frac{e^2}{r_{pm}^3} \tag{3.13}$$

and

$$v'''(r_{pm}) = \frac{1}{6r_{pm}^3}\phi^{(3)} - \alpha_M\frac{e^2}{r_{pm}^4}\ , \tag{3.14}$$

where Eq. (2.4) has been used. The method for determining $\phi^{(2)}$ and $\phi^{(3)}$ is discussed in Sec. II; r_{pm} is determined self-consistently.

D. Dielectric Properties

Potential-minimum values for ϵ_0, ϵ_∞, and ω_0 are needed to determine the potential-minimum frequencies with either the SDD or the ADD model. Such values are not directly measurable, but can be estimated by straight-line extrapolations to $T = 0$ on graphs of experimental values plotted versus temperature. Since we lack the necessary data with which to do such an extrapolation, we have used the 2 °K experimental values of Lowndes and Martin.[9]

The value of the sum of the polarizabilities ($\alpha_+ + \alpha_-$) was determined from the experimental value of the high-frequency dielectric constant ϵ_∞ and the Clausius–Mossotti relation

$$\alpha_+ + \alpha_- = \frac{3}{4\pi}\,\frac{\epsilon_\infty+1}{\epsilon_\infty+2}\,2r^3\ . \tag{3.15}$$

The ratio α_+/α_- was set equal to the ratio of the electronic polarizabilities of K^+ and Br^- given by Tessmann, Kahn, and Shockley.[10] Although ϵ_∞ and r were used in the actual determination of α_+ and α_-, it is more convenient, for the purpose of the discussion here, to think of ϵ_∞ as being determined by α_+, α_-, and r, as indicated in Fig. 1.

The strength of the deformation dipoles is determined by the value of the Szigeti effective charge[11]:

$$e^* = \omega_0\left(\frac{\epsilon_0-\epsilon_\infty}{4\pi}\right)^{1/2}\frac{3}{\epsilon_\infty+2}\,(\bar{M}2r^3)^{1/2}, \tag{3.16}$$

where $\bar{M}$ is the reduced mass of the two ions in a unit cell. The parameters γ and γ' appearing in Fig. 1 were introduced by Hardy[12] to characterize the strength of the deformation dipoles (γ and γ' are not Grüneisen parameters). The long-wavelength optic-mode frequencies depend on γ and γ' only through the combination $\gamma' + 2\gamma$. To obtain the proper values for these frequencies, one sets

$$2(\gamma' + 2\gamma) = e^* - e\ . \tag{3.17}$$

To complete the specification of γ and γ' we set

$$\gamma'/\gamma = rv''(r)/v'(r) \tag{3.18}$$

which, in terms of $A(r)$ and $B(r)$, is

$$\gamma'/\gamma = A(r)/B(r)\ . \tag{3.19}$$

This is somewhat arbitrary, but it is equivalent to the choice suggested by Born and Huang[11] and to that used by Hardy.[12] To be consistent, the zero-pressure value of r at 2 °K, not r_{pm}, has been used in the evaluation of Eqs. (3.15) and (3.16).

E. Determination of $\partial e^*/\partial r$

To determine the mode-Grüneisen parameters with the ADD model requires values for the Szigeti effective charge e^* at both $r = r_{pm}$ and $r = r_{pm} + \Delta r$. We set

$$e^*\big|_{r=r_{pm}+\Delta r} = e^*\big|_{r=r_{pm}}\left[1 + \left(\frac{r}{e^*}\frac{\partial e^*}{\partial r}\right)_{pm}\frac{\Delta r}{r_{pm}}\right] \tag{3.20}$$

and used Eq. (3.16) to determine the potential-minimum value of e^*. To determine $\partial e^*/\partial r$, we used the derivative of Eq. (3.16) with respect to r to relate $\partial e^*/\partial r$ to the derivatives of ϵ_∞, ϵ_0, and ω_0.

It follows from the assumption that the polarizabilities α_+ and α_- are independent of r from the Clausius–Mossotti relation, Eq. (3.15), that

$$\frac{\partial\epsilon_\infty}{\partial r} = -\frac{(\epsilon_\infty-1)(\epsilon_\infty+2)}{r}\ . \tag{3.21}$$

It follows from Eqs. (2.8) and (2.11) that

$$\left(\frac{\partial \epsilon_0}{\partial r}\right)_T = -\frac{3B^{1s}}{r}\left(\frac{\partial \epsilon_0}{\partial P}\right)_T . \quad (3.22)$$

The available experimental values for $(\partial\epsilon_0/\partial P)_T$ are room-temperature values while, to be consistent with the 2 °K data used for ϵ_0, ϵ_∞, and ω_0, the 2 °K value of $(\partial\epsilon_0/\partial P)_T$ is needed. We have used the expression for the pressure dependence of the room-temperature value of $(\partial\epsilon_0/\partial P)_T$ given by Jones[13] and have evaluated it at the pressure $P(2)$ that would be needed to reduce the volume of the crystal at room temperature to the volume it has at 2 °K at zero pressure. This gives the 2 °K value of $(\partial\epsilon_0/\partial P)_T$ at zero pressure to the extent that $\epsilon_0(P, T)$ equals $\epsilon_0(V(P, T))$ or, equivalently, to the extent that $(\partial\epsilon_0/\partial T)_V$ is negligible. The zero-pressure value of $(\partial\epsilon_0/\partial P)_T$ for KBr given by Jones[13] is -5.636×10^{-11} cm^2/dyn. At pressure $P(2)$, which is equal to 3.62×10^9 dyn/cm^2, the value of $(\partial\epsilon_0/\partial P)_T$ is -4.602×10^{-11} cm^2/dyn. Thus, the derivative $(\partial\epsilon_0/\partial P)_T$ is approximately 18% less at 2 °K than it is at room temperature. We have used the quantity $B_0^{1s}+(\partial B^{1s}/\partial P)P(2)$ to estimate the room-temperature value of the bulk modulus at pressure $P(2)$ for use in Eq. (3.22).

The dependence of ω_0 on r is determined by the dependence of $v(r)$, ϵ_∞, and ϵ_0 on r, and by the model. The frequency of the transverse-optic modes at the zone center predicted by the DD model is[14]

$$\omega_{TO}^2 = (e^2/2r^3\bar{M})[A(r)+2B(r)] - (2\pi/9\bar{M}r^3)(\epsilon_\infty+2)(e^*)^2 . \quad (3.23)$$

In principle, ω_{TO} equals the infrared dispersion frequency ω_0 (if one neglects the self-energy frequency shift). Even though the experimental quantity ω_0 enters into the calculation of ω_{TO} through the Szigeti effective charge e^*, the model does not assure that $\omega_{TO}=\omega_0$. Nevertheless, for KBr the calculated quantity ω_{TO} differs from the experimental quantity ω_0 by less than 1% (see Table II).

Since ω_{TO} and ω_0 should be equal, we derived the following expression for ω_0 by substituting Eq. (3.16) into Eq. (3.23), replacing the symbol ω_{TO} with ω_0, using Eqs. (3.7) and (3.8), and solving the resulting expression for ω_0^2:

$$\omega_0^2 = (2/\bar{M})[v''(r)+2r^{-1}v'(r)][(\epsilon_\infty+2)/(\epsilon_0+2)]. \quad (3.24)$$

This reduces to the first Szigeti relation[11] in the potential-minimum configuration. The derivative of Eq. (3.24) with respect to r was used to relate $\partial\omega_0/\partial r$ to the derivatives of $v(r)$, ϵ_∞, and ϵ_0.

By differentiating Eq. (3.16) with respect to r, solving for $\partial e^*/\partial r$, and using the above results for the derivatives of ϵ_∞, ϵ_0, and ω_0, we arrived at the expression

$$\left(\frac{r}{e^*}\frac{\partial e^*}{\partial r}\right)_{pm} = \frac{3}{2} + \frac{r^2v''' + 2(rv'' - v')}{2(rv''+2v')} - \frac{3(\epsilon_\infty+2)}{2(\epsilon_0+2)(\epsilon_0-\epsilon_\infty)}\left[B_0^{1s} + \left(\frac{\partial B^{1s}}{\partial P}\right)_T P(2)\right] \times\left(\frac{\partial \epsilon_0}{\partial P}\right)_T + \frac{(\epsilon_0+2)(\epsilon_\infty-1)}{2(\epsilon_0-\epsilon_\infty)} . \quad (3.25)$$

When evaluating this, we used the potential-minimum values of r, v', v'', and v''', the 2 °K values of ϵ_0 and ϵ_∞, the room-temperature values of B_0^{1s} and $(\partial B^{1s}/\partial P)_T$, and the room-temperature value of $(\partial\epsilon_0/\partial P)_T$ at pressure $P(2)$. Our value of 0.98 for the quantity

$$\frac{\partial \ln e^*}{\partial \ln V} = \frac{r}{3e^*}\frac{\partial e^*}{\partial r} \quad (3.26)$$

is in good agreement with the values of 0.98 and 0.90 estimated by Lowndes,[15] but is quite different from the value of −0.05 estimated by Barron and Batana.[16]

F. Determination of r_{pm}

The value of the distance between nearest neighbors in the potential-minimum configurations r_{pm} is needed for the model determination of the frequencies and mode-Grüneisen parameters. The zero-pressure value of the distance between neares neighbors $r_0(T)$ can be determined experimentally but, because of the zero-point motion in real crystals, r_{pm} is never equal to $r_0(T)$, even at absolute zero.

We have used a self-consistent procedure to determine r_{pm}. We have varied r_{pm} until our predicted value for $r_0(T)$ at room temperature is in agreement with the experimental value. The predicted value for $r_0(T)$ is determined by the value of $u_0(T)$ and the relation

$$r_0(T) = r_{pm}[1+u_0(T)] , \quad (3.27)$$

which follows from Eq. (2.3) and the definition of $u_0(T)$. Equation (2.19) determined $u_0(T)$.

Our final values for $r_0(T)$ predicted with the ADD model are given in Fig. 2. Our final value for $r_0(T)$ at $T=298$ °K for the ADD model is 3.2999×10^{-8} cm; the corresponding experimental value is 3.3000×10^{-8} cm.[17] The self-consistent procedure was carried out for the ADD model only. The value of r_{pm} determined with that model was also used with the RI and SDD models.

IV. RESULTS AND COMPARISON WITH EXPERIMENT

A. Mode-Grüneisen Parameters

The mode-Grüneisen parameters $\gamma_{\vec{k}s}$ determined with the RI, SDD, and ADD models for $\vec{k}$ vectors in three directions of high symmetry are given in

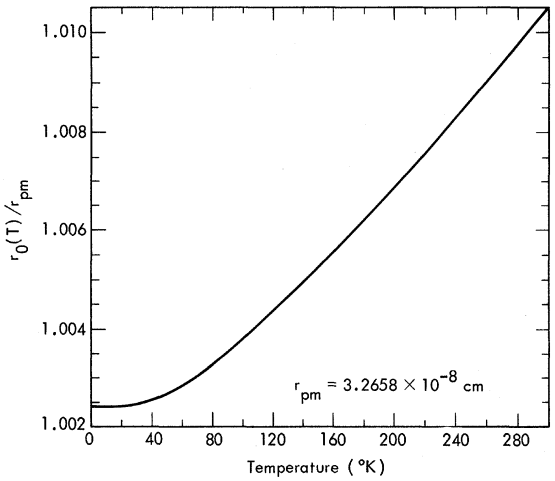

FIG. 2. Temperature dependence of the distance between nearest neighbors at zero pressure for KBr as predicted with the ADD model.

Fig. 3.[18] A brief inspection of the figure reveals appreciable differences between the predictions of the three models. This suggests that comparing the calculated and experimentally determined values for the mode-Grüneisen parameters should be a sensitive way to determine the accuracy of an anharmonic model. Unfortunately, little experimental information is available for such a comparison, except for modes with $\vec{k}$ vectors near the center of the Brillouin zone. Nevertheless, our ADD-model values for $\gamma_{\vec{k}s}$ are in reasonable agreement with the results of other researchers[1,3,19] (in particular, see Fig. 3 of Ruppin and Roberts[3]).

The experimental parameters that determine the frequencies of modes near the center of the zone are the elastic constants C_{11}, C_{12}, and C_{44}, the infrared dispersion frequency ω_0, and the dielectric constants ϵ_0 and ϵ_∞. Since $\gamma_{\vec{k}s} = -(V/\omega_{\vec{k}s}) \times (\partial\omega_{\vec{k}s}/\partial V)$, and since experimentally the volume is varied by varying the pressure, the pressure derivatives of C_{11}, C_{12}, C_{44}, ω_0, ϵ_0, and ϵ_∞ are the essential experimental parameters for determining the zone-center mode-Grüneisen parameters. Model and experimental values for some of these parameters are given for comparison in Table II. The agreement between the values predicted by the ADD model and the experimental values is quite satisfactory. The most serious discrepancy is probably in the values for C_{44} and $(\partial C_{44}/\partial P)_T$. discrepancy is probably in the values for C_{44} and $(\partial C_{44}/\partial P)_T$.

Both the RI and the DD models predict the same elastic behavior. The model values for C_{11}, C_{12}, and C_{44} were determined with standard formulas,[20] while the experimental potential-minimum values were determined by making straight-line extrapo-

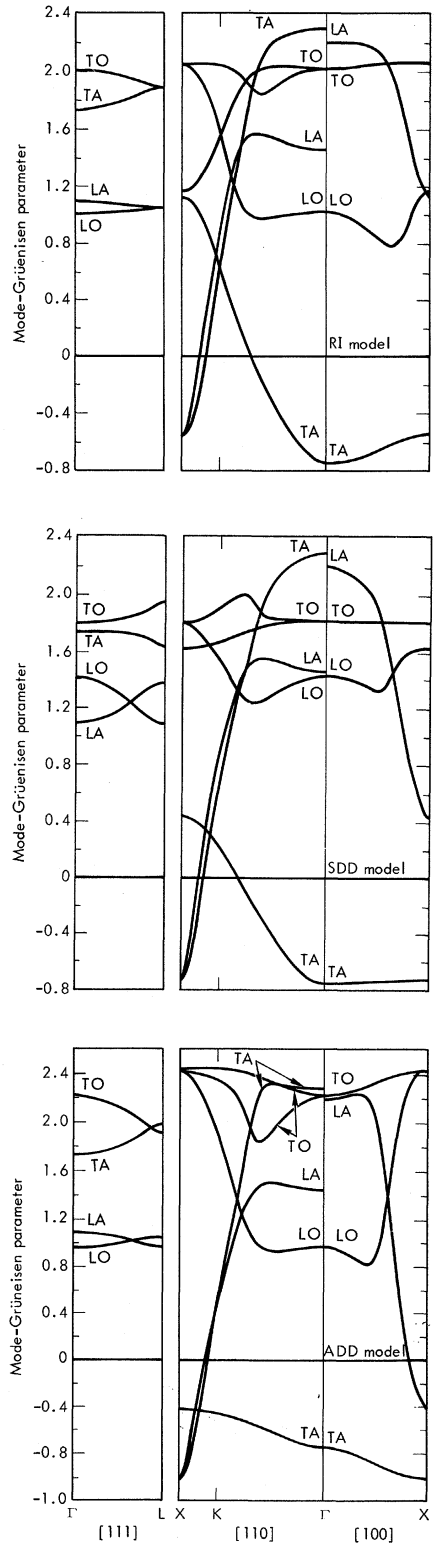

FIG. 3. Mode-Grüneisen parameters for KBr along the [1,1,1], [1,1,0], and [1,0,0] directions in $\vec{k}$ space as predicted by the RI, SDD, and ADD models. The symbols Γ, L, X, and K designate the points of high symmetry in the first Brillouin zone of the fcc lattice.

TABLE II. Model and experimental values of properties that determine $\omega_{\vec{k}s}$ and $\gamma_{\vec{k}s}$ with $\vec{k}=0$ for KBr. The notation pm is used to label potential-minimum values. All values are in cgs units.

Property	Model value		Experimental value	
B_{pm}	1.772×10^{11}	(pm)	1.772×10^{11}	(extrapolated)
$(\partial B^{is}/\partial P)_T$	5.331	(300 °K)	5.331[a]	(300 °K)
	4.479	(ppm)		
C_{11}	3.906×10^{11}	(pm)	4.277×10^{11}	(extrapolated)
C_{12}	0.705×10^{11}	(pm)	0.56×10^{11}	(extrapolated)
C_{44}	0.705×10^{11}	(pm)	0.52×10^{11}	(extrapolated)
$(\partial C_{11}/\partial P)_T$	10.38	(pm)	12.91[a]	(300 °K)
$(\partial C_{12}/\partial P)_T$	1.53	(pm)	1.542[a]	(300 °K)
$(\partial C_{44}/\partial P)_T$	−0.469	(pm)	−0.328[a]	(300 °K)
$(\partial\epsilon_\infty/\partial P)_T$	13.64×10^{-12}	(300 °K, ADD)	9.92×10^{-12}[b]	(300 °K)
ω_{TO}	2.309×10^{13}	(pm, DD)	2.32×10^{13}[c]	(2 °K)
	2.187×10^{13}	(pm, RI)		
γ_{TO}	2.221	(pm, ADD)	2.83[d]	
	1.802	(pm, SDD)	1.59[e]	
	2.009	(pm, RI)		

[a]P. J. Reddy and A. L. Ruoff (Ref. 8).
[b]R. M. Waxler and C. E. Weir, J. Res. Natl. Bur. Stand. 69A, 325 (1965).
[c]R. P. Lowndes and D. H. Martin (Ref. 9).
[d]C. Postmus and J. R. Ferraro, Phys. Rev. 174, 983 (1968).
[e]R. P. Lowndes (Ref. 15).

lations to $T=0$ on elastic-constant—versus—temperature plots. Since the input parameters were determined so that the model and experimental values for B_{pm} agreed, and since $3B=(C_{11}+2C_{12})$, the overestimate of C_{12} by a model is necessarily associated with an underestimate of C_{11}.

The model values of the pressure derivatives of the elastic constants $C_{\mu\nu}$ were determined with

$$\left(\frac{\partial C_{\mu\nu}}{\partial P}\right)_{pm} = -\frac{\gamma_{pm}}{3B_{pm}}\left.\frac{\partial C_{\mu\nu}}{\partial\gamma}\right|_{\gamma=\gamma_{pm}} \qquad (4.1)$$

and the standard formulas for the elastic constants.[20] The fact that only room-temperature experimental values are available for comparison with the potential-minimum model values makes the significance of the comparison somewhat uncertain. An idea of the difference that can exist between room-temperature and potential-minimum values of the pressure derivatives can be obtained from the two model values for $(\partial B^{is}/\partial P)_T$ given in Table II. The exact agreement between the model and experimental values of $(\partial B^{is}/\partial P)_T$ at 300 °K is assured by the method used to determine the input parameters.

The ADD-model value for $\partial\epsilon_\infty/\partial P$ at $T=300$ °K was calculated with

$$\left(\frac{\partial\epsilon_\infty}{\partial P}\right)_T = -\frac{\gamma_0(T)}{3B_0^{is}(T)}\left.\frac{\partial\epsilon_\infty}{\partial\gamma}\right|_{\gamma=\gamma_0(T)} . \qquad (4.2)$$

Equation (3.21) and the Clausius-Mossotti relation were used to determine $\partial\epsilon_\infty/\partial\gamma$.

B. Thermal Expansion

Since no information about the thermal expansion of the crystal was used in setting up the models or in determining the input parameters, it is meaningful to test the models by comparing the predicted and experimental values of either the linear coefficient of thermal expansion $\alpha(T)$ or the macroscopic Grüneisen function,

$$\gamma(T)=3\alpha(T)B^{is}(T)V(T)/C_V(T). \qquad (4.3)$$

When presenting results graphically, a more sensitive comparison of the low-temperature behavior can be obtained with $\gamma(T)$ than with $\alpha(T)$. Model and experimental values for $\gamma(T)$ are given in Fig. 4. The experimental points were determined from the thermal-expansion data of Meincke and Graham,[21] the specific-heat data of Berg and Morrison,[22] and the elastic-constant data of Sharko and Botaki.[7]

The ADD-model values for the macroscopic Grüneisen function at zero pressure, $\gamma_0(T)$, which are given in Fig. 4, were calculated with

$$\gamma_0(T)=\frac{3\alpha_0(T)B_0^{is}(T)V_{pm}[1+u_0(T)]^3}{C_V(V_{pm},T)}, \qquad (4.4)$$

where Eq. (2.8) has been used. The linear coefficient of thermal expansion at zero pressure is

$$\alpha_0(T)=\frac{1}{\gamma_0(T)}\frac{d\gamma_0(T)}{dT} . \qquad (4.5)$$

By differentiating Eq. (2.19) with respect to T, and using Eqs. (3.27) and (4.5), one can show that

$$\alpha_0(T) = \frac{1}{3B_0^{1s}(T)} \times\left(\frac{1}{1+u_0(T)}\frac{\partial P_{th}(T)}{\partial T} - 3u_0(T)\frac{\partial B_0^{1s}(T)}{\partial T}\right) \times\left[1+u_0(T)\left(2-\frac{\phi^{(3)}}{18r_{pm}^3 B_0^{1s}(T)}\right)\right]^{-1}. \quad (4.6)$$

It follows from Eq. (2.6) that

$$\frac{\partial P_{th}(T)}{\partial T} = \frac{1}{(2\pi)^3}\sum_s \int d^3k\, C_{\vec{k}s}(T)\gamma_{\vec{k}s}\ , \quad (4.7)$$

where the heat capacity per mode is

$$C_{\vec{k}s}(T) = \frac{1}{4k_B T^2}\left(\frac{\hbar\omega_{\vec{k}s}}{\sinh(\hbar\omega_{\vec{k}s}/2k_B T)}\right)^2. \quad (4.8)$$

In calculating the heat capacity, we have neglected the contributions of the terms in Eq. (2.2) containing $f^{(1)}(T)$ and $f^{(2)}(T)$ and used the value

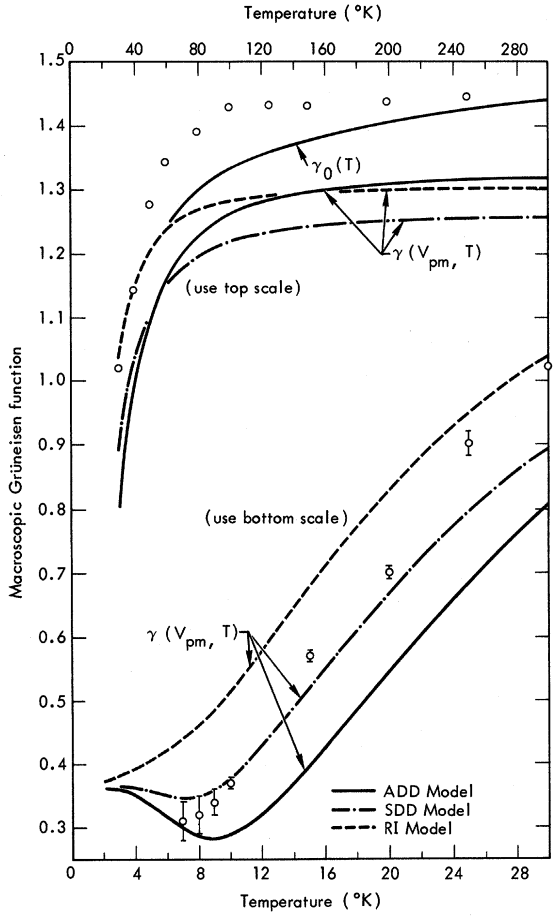

FIG. 4. Macroscopic Grüneisen function for KBr. The circles (○) indicate experimental values of $3\alpha B^{1s}V/C_V$. The lines represent values of $\gamma_0(T)$ or $\gamma(V_{pm}, T)$ determined with Eq. (4.4) or Eq. (4.11), respectively.

$$C_V(V_{pm}, T) = \frac{V_{pm}}{(2\pi)^3}\sum_s \int d^3k\, C_{\vec{k}s}(T)\,, \quad (4.9)$$

which is the value appropriate to the volume $V = V_{pm}$ when self-energy contributions are neglected.

If one sets $u_0(T) = 0$ on the right-hand side of Eq. (4.6), one would obtain an expression of the form

$$\alpha(V_{pm}, T) = \frac{1}{3B^{1s}(T)}\frac{\partial P_{th}(T)}{\partial T}\ . \quad (4.10)$$

As the notation indicates, this is the value of $\alpha(T)$ appropriate to the pressure $P_{th}(T)$ that reduces the volume of the system at temperature T to the potential-minimum value V_{pm} provided, of course, that the value of $B^{1s}(T)$ appropriate to that pressure is used. The macroscopic Grüneisen function for temperature T and pressure P_{th} is

$$\gamma(V_{pm}, T) = \left(\sum_s \int d^3k\, C_{\vec{k}s}(T)\gamma_{\vec{k}s}\right) \Big/ \left(\sum_s \int d^3k\, C_{\vec{k}s}(T)\right), \quad (4.11)$$

which is a special case of Eq. (1.2). Expressions of this form are often used to calculate values for the macroscopic Grüneisen function, which are then compared with zero-pressure experimental values.

Equation (4.11) was used to determine the RI-, SDD-, and ADD-model values of $\gamma(V_{pm}, T)$ given in Fig. 4. By utilizing a scheme for evaluating integrals over the first Brillouin zone that divides the zone into several distinct concentric regions and samples the integrand at a higher density of points in the region at the center of the zone, we have obtained values for $\gamma(V_{pm}, T)$ that we estimate are accurate to better than 1% at temperatures as low as 3 °K. This has enabled us to show unambiguously that well-defined minima exist in the values of the macroscopic Grüneisen function predicted by the ADD and SDD models, but not in the values predicted by the RI model.

It is apparent from Fig. 4 that the ADD-model values for $\gamma_0(T)$ are in better agreement with the experimental values than the values for $\gamma(V_{pm}, T)$. In particular, at 250 °K the zero-pressure macroscopic Grüneisen function $\gamma_0(T)$ is only 1.4% less than the experimental value, while $\gamma(V_{pm}, T)$ is 9% less. Of course, this is not surprising, since the experimental points were calculated with zero-pressure data.

Although the ADD-model value for $\gamma_0(T)$ is very close to the experimental value at 280 °K, the model values drop appreciably below the experimental values at lower temperatures. To see which one of the parameters in Eq. (4.3) contributes most to this discrepancy, we have calculated the ratios of the model values to the experimental values of $\alpha_0(T)$, $B_0^{ad}(T)$, and $C_V(T)$ and have presented the results in Fig. 5. This method for presenting the data em-

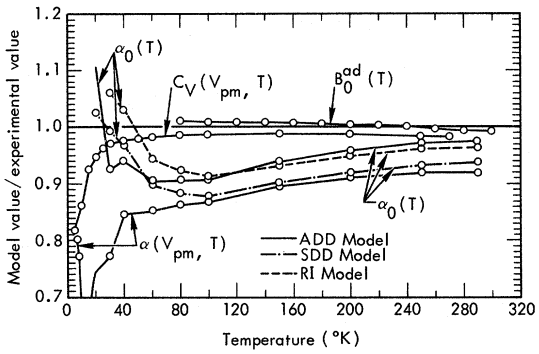

FIG. 5. Temperature dependence for KBr of the ratio of the model value divided by the experimental value of the adiabatic bulk modulus B^{ad}, the heat capacity C_V, and the linear coefficients of thermal expansion $\alpha_0(T)$ and $\alpha(V_{pm}, T)$ determined with Eqs. (4.6) and (4.10), respectively.

phasizes any differences that exist between the experimental and model values of $\alpha_0(T)$ and $C_V(T)$ at low temperatures.

It is readily seen from Fig. 5 that the major source of the discrepancy between the model and experimental value for $\gamma_0(T)$ is in the determination of the coefficient of thermal expansion. The ADD values for the heat capacity $C_V(V_{pm}, T)$ are within 2 °K of the experimental value at temperatures above 50 °K, despite the fact that the anharmonic contributions are neglected. The model values for $B_0^{is}(T)$ are in good agreement with the experimental values at temperatures above 80 °K. Unfortunately, reliable experimental values for $B_0^{is}(T)$ below 80 °K are not available. Even though Eq. (2.10) gives reliable estimates for $B_0^{is}(T)$, it does not give reliable estimates for $(\partial B^{is}/\partial T)_P$ at low temperatures. In particular, it is the poor estimate of $(\partial B^{is}/\partial P)_P$ that causes the model value for $\alpha_0(T)$ to exceed the experimental value at the lower temperatures.

The ADD-model values for $\alpha(V_{pm}, T)$ are also given in Fig. 5 to illustrate the significance of the corrections to Eq. (4.10) that are included in the complete expression (4.6). [The zero-pressure values for $B^{is}(T)$ were used in determining the values of $\alpha(V_{pm}, T)$ given in the figure.] The corrections increase the ADD-model value of the coefficient of thermal expansion by approximately 5% at temperatures above 80 °K. Below 80 °K, it is difficult to estimate the significance of the corrections because of the lack of reliable values for $(\partial B^{is}/\partial T)_P$.

V. DISCUSSION AND CONCLUSIONS

A. Consistent Use of Models

One reason for creating crystal models is to help determine the nature of the microscopic interactions in real crystals. If a model predicts values for several independent properties that are in good agreement with experimental values, one feels reasonably confident in assuming that the interactions allowed for in the model at least approximate those in the real crystal, and one then hopes that the model will be capable of predicting crystal properties that are not already known. Of course, for any such predictions to be reliable, the model must be used consistently. In particular, the same interactions, and interactions of the same strength, must be used in all of the predictions made. Also, all of the effects of each of the interactions included in a model should be considered.

Consider the often used procedure of determining the strength of the overlap forces by substituting room-temperature zero-pressure data into formulas derived using the equilibrium condition. Since a real crystal at room temperature is not in a configuration in which the electrostatic forces exactly balance the overlap forces because of thermal expansion, it is certainly not strictly consistent to use such a procedure. Nevertheless, one might hope that the errors introduced by using the procedure would be negligible. To check whether or not this is the case, we have calculated values for the first two derivatives of the nearest-neighbor overlap potential $v(r)$ both by substituting room-temperature data directly into formulas derived using the equilibrium condition, and by taking into account the effects of thermal expansion, etc. The results are given in Table III.

Formulas (2.14), (3.12), and (3.13) were derived using the equilibrium condition. They are equivalent to the expressions given by Kellermann[23] for determining the dimensionless parameters $B(r)$ and $A(r)$ related to $v'(r)$ and $v''(r)$. Within the harmonic approximation, which was being considered by Kellermann, it is consistent to substitute room-temperature zero-pressure experimental data into these formulas, since in the harmonic approximation there is neither thermal expansion to cause the distance between nearest neighbors at zero pressure $r_0(T)$ to differ from potential-minimum distance r_{pm}, nor temperature dependence in the elastic constants to cause the zero-pressure bulk modulus $B_0^{is}(T)$ to differ from the potential-minimum value B_{pm}. Only in the potential-minimum configuration do the electrostatic forces exactly balance the overlap forces.

The values given in Table III for $v'(r)$ and $v''(r)$ at $r = r_{pm}$ were determined by substituting actual potential-minimum data into Eqs. (2.14), (3.12), and (3.13). The potential-minimum distance r_{pm} was determined self-consistently (see Sec. III), while B_{pm} was determined by an extrapolation of the experimental data (see Sec. II). The "consistent" values for $v'(r)$ and $v''(r)$ at the nearest-neighbor distance $r_0(T)$ were determined with

TABLE III. Values for KBr of the first two derivatives of the interaction potential $v(r)$ associated with the overlap forces acting between nearest neighbors. The "consistent" values were calculated with formulas that allow for the effects of thermal expansion, etc. The "approximate" values were calculated with formulas derived using the equilibrium condition.

Distance between neighbors	Comment	$v'(r)$ (erg/cm)	$v''(r)$ (erg/cm^2)
$r=r_{pm}$		-6.300×10^{-5}	2.122×10^{4}
$r=r_0(1\,^\circ\mathrm{K})$	consistent	-6.136×10^{-5}	2.076×10^{4}
	approximate	-6.270×10^{-5}	2.092×10^{4}
	2% difference		0.8% difference
$r=r_0(300\,^\circ\mathrm{K})$	consistent	-5.607×10^{-5}	1.920×10^{4}
	approximate	-6.170×10^{-5}	1.783×10^{4}
	10% difference		7% difference

$$v'(r_0(T)) = v'(r_{pm}) + v''(r_{pm})\,[r_0(T) - r_{pm}] + \tfrac{1}{2}v'''(r_{pm})[r_0(T) - r_{pm}]^2 \quad (5.1)$$

and

$$v''(r_0(T)) = v''(r_{pm}) + v'''(r_{pm})\,[r_0(T) - r_{pm}]\,. \quad (5.2)$$

The "approximate" values for $v'(r)$ and $v''(r)$ at $r=r_0(T)$ were determined by substituting the zero-pressure values of $r_0(T)$ and $B_0^{is}(T)$ (instead of r_{pm} and B_{pm}) into formulas (2.14), (3.12), and (3.13). It can be seen from the table that the substitution of room-temperature zero-pressure experimental data directly into these formulas leads to a 10% overestimate of the magnitude of $v'(r_0(300\,^\circ\mathrm{K}))$ and a 7% underestimate of the value of $v''(r_0(300\,^\circ\mathrm{K}))$. If one is seeking to construct models that accurately reflect the microscopic properties of real crystals, these errors are certainly significant. As one expects, the errors resulting from the use of 2 °K experimental data are much smaller.

Significant errors also result if one is not careful to consider all of the effects of including an overlap potential $v(r)$ with a nonzero third derivative. The derivative $v'''(r_{pm})$ is an essential parameter for determining the value of both $f^{(1)}(T)$ and $\phi^{(3)}$, which occur in the free-energy expansion (2.2). The coefficient $f^{(1)}(T)$ is proportional to the thermal pressure $P_{th}(T)$ and is determined by the values of the mode-Grüneisen parameters, while $\phi^{(3)}$ contributes to the temperature dependence of the bulk modulus $B_0^{is}(T)$. The major contribution to the coefficient of thermal expansion $\alpha_0(T)$ is from $(1/3B^{is})\,(\partial P_{th}/\partial T)$. Nevertheless, to include all of the effects of allowing $v(r)$ to have a nonzero third derivative, one must also include the contributions to $\alpha_0(T)$ of the terms in Eq. (4.6) that involve $[\partial B_0^{is}(T)/\partial T]_P$ and $\phi^{(3)}$. One might hope that the error introduced by neglecting such terms would be negligible, but, as pointed out in Sec. IV, including them appreciably increases the predicted values of both $\alpha_0(T)$ and $\gamma_0(T)$ and significantly improves the agreement with experiment. It is reasonable to expect that the contributions of such terms will be of roughly the same relative size in other alkali halides.

Finally, we would like to mention a few ways in which a model can inadvertently be used inconsistently. To determine the mode-Grüneisen parameters $\gamma_{\vec{k}s}$ one needs the values of the volume derivatives of the normal-mode frequencies $\omega_{\vec{k}s}$. One of the simplest methods for determining these derivatives is to calculate the difference between the frequencies predicted with two different sets of input parameters and use Eq. (3.2). The two sets of input parameters correspond to slightly different volumes. The differences between the sets can be determined from the experimental values of the pressure derivatives. However, it would not be consistent to employ two such sets of input parameters in a computer program that uses the harmonic approximation to determine the frequencies directly from the basic experimental data: Most such programs employ the equilibrium condition. If the equilibrium condition is satisfied at one of the values of the volume, it necessarily cannot be satisfied at the other value.

B. RI and SDD Models

One of the shortcomings of the RI model is its failure to predict the ratio ω_{LO}/ω_{TO} correctly, where ω_{LO} and ω_{TO} are the long-wavelength longitudinal- and transverse-optic-mode frequencies, respectively. The DD model corrects for this shortcoming. Nevertheless, the RI model predicts values for $\alpha_0(T)$ that are in better agreement with experiment than the predictions of the SDD model (see Fig. 4). Since both models allow for the same anharmonicity, while the SDD model predicts the harmonic properties more accurately, we conclude that the relative success of the RI model must be the result of the errors caused by the shortcomings of the harmonic aspects of the model being cancelled by the errors caused by the incompleteness of the anharmonic aspects of the model.[24]

C. ADD Model

The ADD model used here predicts results that agree reasonably well with the experimental data, particularly when one considers the simplicity of

the model and the small number of parameters determined from experimental data. Since no information about $\alpha_0(T)$ was used in setting up the model, the ability of our model to predict a value of $\alpha_0(T)$ at 290°K that is within 3% of the experimental value is quite satisfying. Nevertheless, the larger discrepancies between the predicted and experimental values at lower temperatures (see Fig. 5) indicate that the model still needs considerable refining. Probably the most serious shortcomings of the ADD model, as used here, are its neglect of the coefficient $\phi^{(4)}$ in the expansion of the free energy and its failure to accurately approximate the experimental values of C_{44} and $(\partial C_{44}/\partial P)_T$. If known, the second pressure derivative of the bulk modulus could be used to determine $\phi^{(4)}$, while agreement with the experimental values of C_{44} and $\partial C_{44}/\partial P$ could be obtained by including next-nearest-neighbor overlap forces in the model.

†Work performed under the auspices of the U. S. Atomic Energy Commission.

[1]E. R. Cowley and R. A. Cowley, Proc. R. Soc. A **287**, 259 (1965).
[2]B. N. N. Achar and G. R. Barsch, Phys. Rev. B **3**, 4352 (1971); B. N. N. Achar and G. R. Barsch, Phys. Status Solidi A **6**, 247 (1971).
[3]R. Ruppin and R. W. Roberts, Phys. Rev. B **3**, 1406 (1971).
[4]K. V. Namjoshi, S. S. Mitra, and J. F. Vetelino, Phys. Rev. B **3**, 4398 (1971); J. F. Vetelino, K. V. Namjoshi, and S. S. Mitra, J. Appl. Phys. **41**, 5141 (1970).
[5]R. J. Hardy and A. M. Karo, J. Appl. Phys. **41**, 5144 (1970).
[6]J. K. Galt, Phys. Rev. **73**, 1460 (1948).
[7]A. V. Sharko and A. A. Botaki, Sov. Phys.-Solid State **12**, 1796 (1971).
[8]P. J. Reddy and A. L. Ruoff, in *Physics of Solids at High Pressure*, edited by C. T. Tomizuka and R. M. Emrick (Academic, New York, 1965), p. 510.
[9]R. P. Lowndes and D. H. Martin, Proc. R. Soc. A **308**, 473 (1969).
[10]J. R. Tessman, A. H. Kahn, and W. Shockley, Phys. Rev. **92**, 890 (1953).
[11]M. Born and K. Huang, *Dynamical Theory of Crystal Lattices* (Oxford U. P., Oxford, England, 1954), pp. 82–116.
[12]J. R. Hardy, Philos. Mag. **7**, 315 (1962).
[13]B. W. Jones, Philos. Mag. **16**, 1085 (1967).
[14]S. S. Jaswal and J. R. Hardy, Phys. Rev. **171**, 1090 (1968).
[15]R. P. Lowndes, in *Phonons*, edited by M. A. Nusimovici (Flammarion, Paris, 1971), p. 473.
[16]T. H. K. Barron and A. Batana, Philos. Mag. **20**, 619 (1969).
[17]R. W. G. Wyckoff, *Crystal Structures* (Interscience, New York, 1963), Vol. I, p. 87.
[18]The average value of the mode-Grüneisen parameters (averaged over the six possible values of the polarizing index, and over a uniformly distributed set of $\vec{k}$ values) is 1.30 for the RI model, 1.26 for the SDD model, and 1.32 for the ADD model.
[19]G. R. Barsch and B. N. N. Achar, Phys. Status Solidi **35**, 881 (1969).
[20]R. A. Cowley, Proc. R. Soc. A **268**, 121 (1962).
[21]P. P. M. Meincke and G. M. Graham, Can. J. Phys. **43**, 1853 .
[22]W. T. Berg and J. A. Morrison, Proc. R. Soc. A **242**, 467 (1957).
[23]E. W. Kellermann, Philos. Trans. R. Soc. Lond. A **238**, 513 (1940).
[24]Achar and Barch (Ref. 2) report a similar cancellation of errors in their RI-model calculations for NaCl.

PHYSICAL REVIEW B VOLUME 7, NUMBER 10 15 MAY 1973

Monte Carlo Calculations for Solid and Liquid Argon*

J. A. Barker
IBM Research Laboratory, San Jose, California 95114

M. L. Klein
National Research Council of Canada, Ottawa, Ontario KlA OR6, Canada

(Received 30 October 1972)

Monte Carlo methods are used to evaluate pressure, energy, and specific heat for solid and liquid argon for volumes and temperatures at or near melting. The potential energy is assumed to be the sum of pair-wise-additive potentials recently determined by Barker and co-workers plus the Axilrod–Teller three-body interaction. Quantum corrections are included. The agreement with presently available high-pressure data is excellent.

I. INTRODUCTION

The dynamical behavior of solids with large-amplitude motions is an active area of contemporary solid-state physics, and all the powerful and elegant techniques of many-body theory have been applied to this problem,[1] as well as Monte Carlo[2,3] and molecular dynamics techniques[4] that had proved so successful for fluids. At the same time, the problem of the interatomic forces between simple